Multiply everything by Wij, phi goes away, right side becomes 0?

Supplementary Materials

0.1 Preprocessing expression data

We removed the gene expression profiles with overall small absolute values less than a percentile cutoff (60% is used here). Further, we removed the gene expression profiles with a variance less than the percentile specified by another cutoff (30% is used here). The procedure was done using the standard functions (genelowvalfilter(Data,'Percentile',60) and genevarfilter(Data, 'Percentile',30)) in the Matlab software.

0.2 The SNMNMF algorithm and the discussion of its convergence

The SNMNMF algorithm minimizes the following objective function:

$$\begin{aligned}\mathcal{F}(W,H_1,H_2) = &\sum_{I=1,2}\|X_I - WH_I\|_F^2 \\ &- \lambda_1 Tr(H_2AH_2^T) - \lambda_2 Tr(H_1BH_2^T) \\ &+ \gamma_1\|W\|_F^2 + \gamma_2(\sum_j \|h_j\|_1^2 + \sum_{j'}\|h_{j'}\|_1^2)\end{aligned} \tag{1}$$

with the constraints $W \geq 0$, $H_I \geq 0$ and $I = 1, 2$, where h_j and $h_{j'}$ are the jth and j'th column of H_1 and H_2 respectively.

We expand the popular multiplicative updating algorithm developed for NMF and its variants to SNMNMF. For the NMF problem, although the objective function of NMF is convex in W only or H only, it is not convex in both variables together. Therefore it is unrealistic to expect an algorithm to find the global minimum. The same applies to the SNMNMF problem. Below we detail the multiplicative updating algorithm for SNMNMF to identify the local minimum of $\mathcal{F}$.

Based on the simple knowledge of linear algebra, the objective function $\mathcal{F}$ can be reformulated as follows:

$$\begin{aligned}\mathcal{F} = &\sum_{I=1}^{2}\left[Tr(X_IX_I^T) - 2Tr(X_IH_I^TW^T) + Tr(WH_IH_I^TW^T)\right] \\ &- \lambda_1 Tr(H_2AH_2^T) - \lambda_2 Tr(H_1BH_2^T) \\ &+ \gamma_1 Tr(WW^T) + \gamma_2\sum_{I=1}^{2} e_{1\times k}H_IH_I^Te_{1\times k}^T\end{aligned} \tag{2}$$

. Let ψ_{ij} and ϕ_{ij}^I be the Lagrange multipliers for the constraints $W_{ij} \geq 0$ and $(H_I)_{ij} \geq 0$, respectively. The Lagrange $\mathcal{L}$ is

$$\mathcal{L}(W,H_I) = \mathcal{F} + Tr(\Psi W^T) + \sum_{I=1}^{2} Tr(\Phi_I H_I^T).$$

where $\Psi = [\psi_{ij}]$ and $\Phi_I = [\phi_{ij}^I]$. The partial derivatives of $\mathcal{L}$ with respect to W and H_I are:

$$\frac{\partial\mathcal{L}}{\partial W} = \sum_{I=1}^{2}\left[-2X_IH_I^T + 2WH_IH_I^T\right] + 2\gamma_1 W + \Psi$$

$$\frac{\partial\mathcal{L}}{\partial H_1} = -2W^TX_1 + 2W^TWH_1 - \lambda_2H_2B^T + \gamma_2 2e_{k\times k}H_1 + \Phi_1,$$

$$\frac{\partial\mathcal{L}}{\partial H_2} = -2W^TX_2 + 2W^TWH_2 - \lambda_1 2H_2A - \lambda_2H_1B + \gamma_2 2e_{k\times k}H_2 + \Phi_2,$$

Based on the KKT conditions $\psi_{ij}W_{ij} = 0$ and $\phi_{ij}^I(H_I)_{ij} = 0$, we get the following equations for W_{ij}, $(H_1)_{ij}$ and $(H_2)_{ij}$:

$$-2\sum_{I=1}^{2}(X_IH_I^T)_{ij}W_{ij} + [2\sum_{I=1}^{2}(WH_IH_I^T) + 2\gamma_1 W]_{ij}W_{ij} = 0,$$

$$(-W^TX_1 - \frac{\lambda_2}{2}H_2B^T)_{ij}W_{ij} + (W^TWH_1 + \gamma_2 e_{k\times k}H_1)_{ij}W_{ij} = 0,$$

$$(-W^TX_2 - \lambda_1H_2A - \frac{\lambda_2}{2}H_1B)_{ij}W_{ij} + (W^TWH_2 + \gamma_2 e_{k\times k}H_2)_{ij}W_{ij} = 0.$$

Then we can get the following updating rules:

$$\begin{aligned}w_{ij} &\leftarrow w_{ij}\frac{(X_1H_1^T + X_2H_2^T)_{ij}}{(WH_1H_1^T + WH_2H_2^T + \gamma_1 W)_{ij}}, \\ h_{ij}^1 &\leftarrow h_{ij}^1\frac{(W^TX_1 + \frac{\lambda_2}{2}H_2B^T)_{ij}}{[(W^TW + \gamma_2 e_{k\times k})H_1]_{ij}}, \\ h_{ij}^2 &\leftarrow h_{ij}^2\frac{(W^TX_2 + \lambda_1H_2A + \frac{\lambda_2}{2}H_1B)_{ij}}{[(W^TW + \gamma_2 e_{k\times k})H_2]_{ij}},\end{aligned} \tag{3}$$

We have the following theorem to guarantee the convergence of the above updating rules to a local optimum.

Theorem 1 *The objective function $\mathcal{F}$ of the SNMNMF problem is nonincreasing under the above updating rules. The objective function is finite and invariant under these updates if and only if W, H_1 and H_2 are at a stationary point.*

The principle of convergence proof of NMF can be easily expanded to prove this theorem. A difference to NMF is that the objective function $\mathcal{F}$ here can be unbounded below. Only the objective is finite, the SNMNMF can get a stable local solution. Here, we show that $\mathcal{F}$ is nonincreasing under the updating rules. In particular, here we prove that the $\mathcal{F}$ is nonincreasing under the updating rule for H_1, and same feature under the updating rule for W can be similarly proved. We will adopt the same strategy used in (Lee and Seung, 2001) that introduced an auxiliary function in the Expectation-Maximization algorithm. The following is the definition of the auxiliary function.

Definition *G(h,h') is an auxiliary function for $F(h)$ if the conditions $G(h,h') \geq F(h)$, $G(h,h) = F(h)$ are satisfied.*

Due to the following property, the auxiliary function is very useful for the proof.

Lemma 1 *If G is an auxiliary function of F, then F is nonincreasing under the update $h^{(t+1)} = arg\min G(h, h^{(t)})$.*

With a proper auxiliary function, the updating rule for H_1 is exactly the update in this Lemma. Taking into account any element $(H_1)_{ab}$ in H_I, we use the F_{ab} to denote the part of $\mathcal{F}$ that is only relevant to $(H_1)_{ab}$. It is easy to see that

$$F_{ab}^{'} = \left(\frac{\partial\mathcal{F}}{\partial H_1}\right)_{ab} = (-2W^TX_1 + 2W^TWH_1 - \lambda_2H_2B^T + \gamma_2 2e_{k\times k}H_1)_{ab}$$

$$F_{ab}^{''} = 2(W^TW + \gamma_2 e_{k\times k})_{aa}$$

Because the update is essentially element-wise, it is sufficient to show that each F_{ab} is nonincreasing under the updating rule for H_1.

Lemma 2 *Function*

$$G(h,(H_1)_{ab}^{(t)}) = F_{ab}((H_1)_{ab}^{(t)}) + F'_{ab}((H_1)_{ab}^{(t)})(h-(H_1)_{ab}^{(t)}) + \frac{[(W^TW+\gamma_2 e_{k\times k})H_1]_{ab}}{(H_1)_{ab}^{(t)}}(h-(H_1)_{ab}^{(t)})^2 \quad (4)$$

is an auxiliary function for F_{ab}.

Proof Obviously, $G(h,h) = F_{ab}(h)$. Here we only show that $G(h,(H_1)_{ab}^{(t)}) \geq F_{ab}(h)$. To achieve this, we compare the Taylor series expansion of $F_{ab}(h)$

$$F_{ab}(h) = F_{ab}((H_1)_{ab}^{(t)}) + F'_{ab}((H_1)_{ab}^{(t)})(h-(H_1)_{ab}^{(t)}) + (W^TW+\gamma_2 e_{k\times k})_{aa}(h-(H_1)_{ab}^{(t)})^2 \quad (5)$$

with the auxiliary function $G(h,(H_I)_{ab}^{(t)})$ to find that $G(h,(H_1)_{ab}^{(t)}) \geq F_{ab}(h)$ is equivalent to

$$\frac{[(W^TW+\gamma_2 e_{k\times k})H_1]_{ab}}{(H_1)_{ab}^{(t)}} \geq (W^TW+\gamma_2 e_{k\times k})_{aa}.$$

Obviously, we have

$$((W^TW+\gamma_2 e_{k\times k})H_1)_{ab} = \sum_k (W^TW+\gamma_2 e_{k\times k})_{ak}(H_1)_{kb}^{(t)} \geq (H_1)_{(ab)}^{(t)}(W^TW+\gamma_2 e_{k\times k})_{aa}. \quad (6)$$

Thus $G(h,(H_1)_{ab}^{(t)}) \geq F_{ab}(h)$ holds.

Proof of Theorem 1 We can get the the following updating rule based on the auxiliary function $G(h,(H_1)_{ab}^{(t)})$:

$$(H_1)_{ab}^{(t+1)} = (H_1)_{ab}^{(t)} - (H_1)_{ab}^{(t)}\frac{F'_{ab}((H_1)_{ab}^{(t)})}{2((W^TW+\gamma_2 e_{k\times k})H_1)_{ab}} = (H_1)_{ab}^{(t)}\frac{(W^TX_1+\frac{\lambda_2}{2}H_2B^T)_{ab}}{((W^TW+\gamma_2 e_{k\times k})H_1)_{ab}}. \quad (7)$$

Due to the property of the auxiliary function $G(h,(H_1)_{ab}^{(t)})$ for F_{ab}, F_{ab} is nonincreasing under this updating rule.

0.3 Initialization of the algorithm

We initialize the W, H_1 and H_2 matrices by assigning the uniformly distributed values ranging from 0 to 1 to their entries. We note that, under different runs of the algorithm, the objective function only have minor changes.

0.4 Parameter selection

The method proposed here requires setting of several parameters. Given that 41 miRNAs in the data sets have been previously reported to be related with ovarian cancer (Koturbash *et al*., 2010), and which can have multiple regulatory combination with other miRNAs and the 57 miRNA clusters contained in the data sets (miRNA cluster data from the miRBase website [http://www.mirbase.org/] with a genomic cutoff distance of 50kb, see Materials and Methods), we set the number of co-module to 50. As to the parameters λ_1, λ_2, γ_1, γ_2, they were empirically determined by relative size of each corresponding term of the objective function (Figure S1A). To test the robustness of our result with respect to the initial parameters, we ran our method using several different combinations. We found that more than 60% of the genes were consistently grouped together and most of the enriched terms are the same for these different settings (Figure S1B). Here the consistency measure is defined as the ratio of gene pairs present in the same modules across different results under different settings.

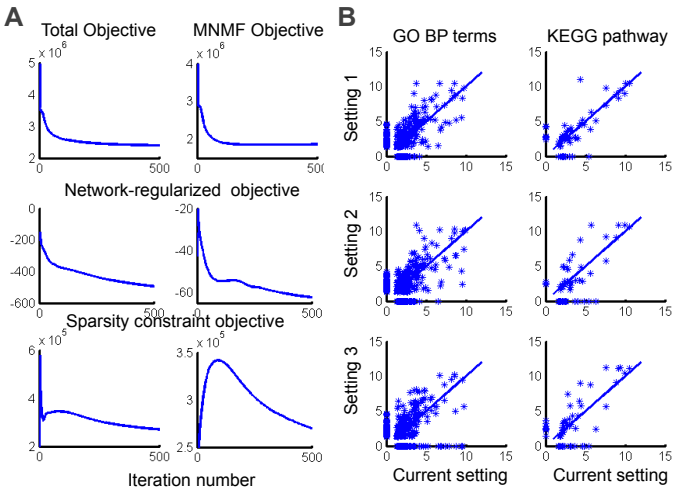

Fig. S1. A. The objective value for current setting. B. Comparison of current parameter setting with other three based on enrichment analysis. The $-log(p\text{-value})$ is shown on x- and y-axis for different parameter settings. There three setting are ($K=50$, $\lambda_1=0.0001$, $\lambda_2=0.01$, $\gamma_1=10$, and $\gamma_2=10$), ($K=50$, $\lambda_1=0.0001$, $\lambda_2=0.01$, $\gamma_1=10$, and $\gamma_2=5$) and ($K=60$, $\lambda_1=0.0001$, $\lambda_2=0.01$, $\gamma_1=10$, and $\gamma_2=5$), respectively.

We have run the programs with different initializations with other fixed parameters, we found that the 90% of the genes were consistently grouped together, indicating the robustness of the method to different initializations.

To select the proper threshold T, we assess the enrichment rate of gene modules with respect to GO biological process. For comparison, the mean rate of functional enrichment for 100 corresponding random runs was also calculated. In Figure S2, we show the ratio of real enrichment rate against the mean of 100 random ones for different cutoff T. The highest peak shows that the $T=7$ is a good threshold.

0.5 Permutation test for between correlations

We show the sum of Pearson's correlation coefficients (PPCs) for the miRNA-gene modules 32 and 40 and their distributions of 1000 random chosen miRNA-gene modules respectively (Figure S3).

0.6 Module size distribution

We run the proposed method on the ovarian cancer dataset and obtained 50 'co-modules' which are composed by a set of miRNAs and a set of genes which are denoted as miRNAs modules and gene modules respectively. We show the module size distribution in Figure S4 and each co-module contains 3.8 miRNAs and 78 genes

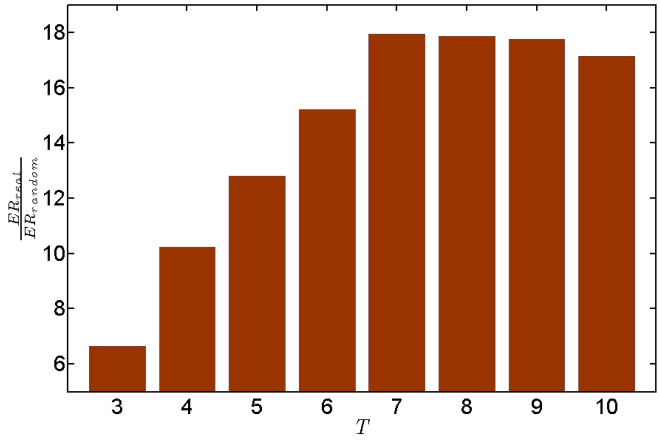

Fig. S2. The distribution of the enrichment ratio of gene modules against the mean of that for modules of 100 random runs under different cutoff T.

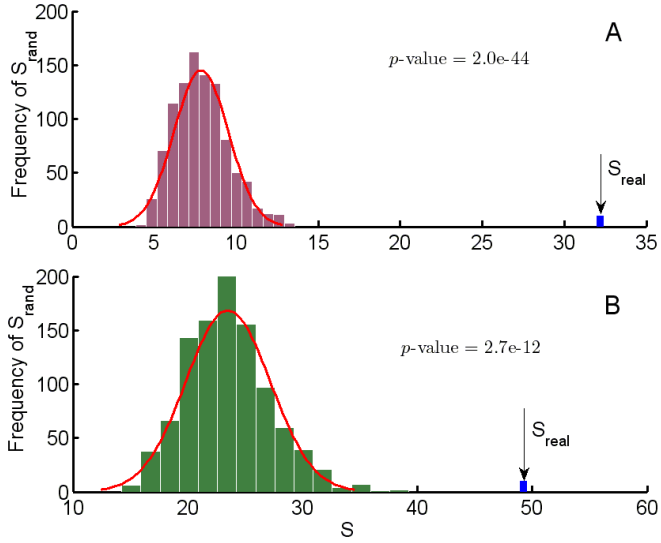

Fig. S3. Distribution of the sum of PCCs of randomly chosen miRNA-gene modules estimated by 1000 random samplings for co-module 32 and 40 respectively.

on average. Note that three miRNAs and one genes modules are empty.

0.7 The literature review support for the overlapping miRNAs

We search any two miRNAs of the overlapping miRNAs for each co-module and see if they are related with the same biological processes uncovered by other studies. The ones supported by literature review were listed in Table S1.

0.8 The co-modules are highly enriched with cancer genes

We listed the modules that are enriched with ovarian cancer genes based on the IPA system in Table S2.

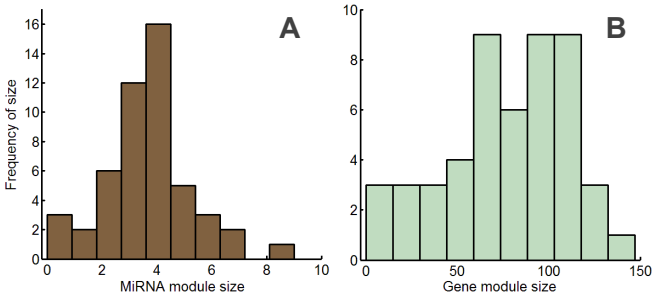

Fig. S4. Module size distribution for miRNA modules and gene modules respectively.

0.9 Illustration of the signals of W basis vectors

Based on the basis matrix W, we can divide the samples into three groups. We show the signals of co-module 39 and 40 with corresponding dividing lines (Figure S5).

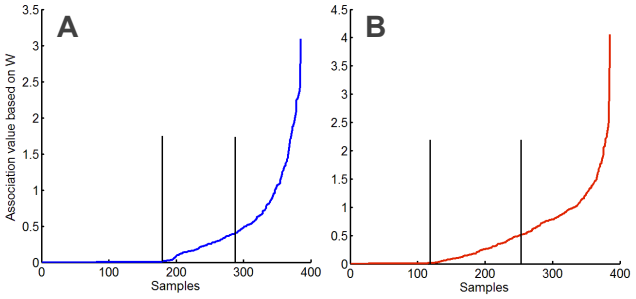

Fig. S5. The signals of W basis vectors for co-module 39 and 40 respectively. The same figure for other co-modules can be similarly plotted.

0.10 The EBC method

The EBC method integrated two types of information to identify miRNA-gene regulatory module. The method has the following major steps (Figure S6): (1) Calculate miRNA-gene correlation matrix based on the (inverse) correlations in the expressions across samples, and convert the correlation matrix into a miRNA-gene correlation network. (2) Construct a miRNA-gene regulatory network by combining the constructed miRNA-gene correlation network and the corresponding predicted miRNA-gene regulatory network. (3) Enumerate all maximal bicliques as candidate regulatory modules, remove the ones with genes less than ten, and postprocess candidate modules.

The maximal bicliques in a bipartite network can have quite big overlap. For example, the maximal biclique 1 and 2 have a large number of overlapping genes, and their combinations and maximal biclique 3 only have two genes difference (Figure S7).

REFERENCES

Yang, X. *et al.* (2009) miR-449a and miR-449b are direct transcriptional targets of E2F1 and negatively regulate pRb-E2F1 activity through a feedback loop by targeting CDK6 and CDC25A. *Genes Dev.*, **23**, 2388-93.

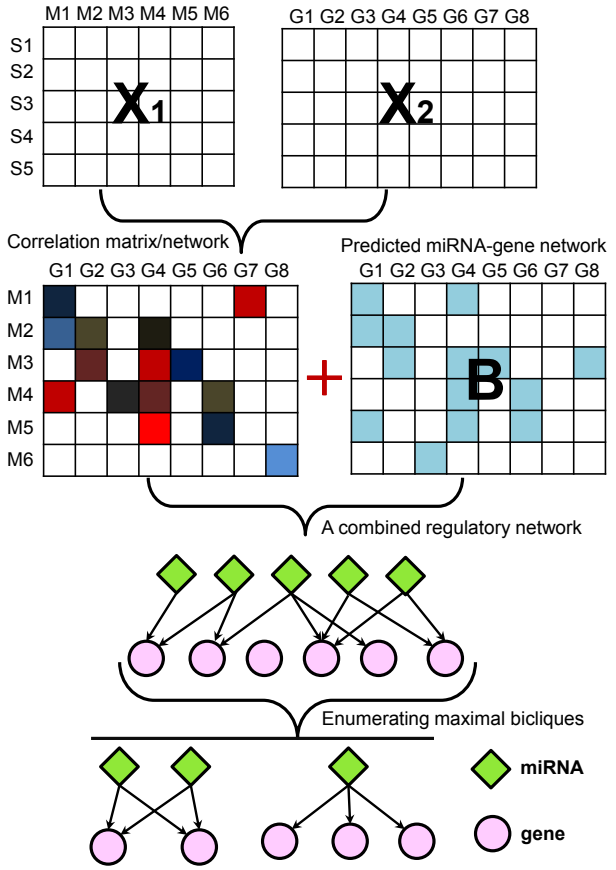

Fig. S6. Workflow of the EBC method for co-module identification.

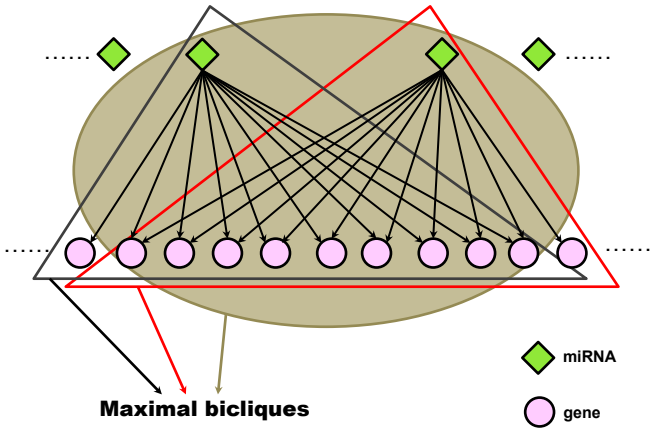

Fig. S7. Examples of maximal bicliques.

Corney, D.C. *et al*. (2007) MicroRNA-34b and microRNA-34c are targets of p53 and cooperate in control of cell proliferation and adhesion-independent growth. *Cancer Res*., **67**, 8433-8.

Kent, O.A. *et al*. (2010) Repression of the miR-143/145 cluster by oncogenic Ras initiates a tumor-promoting feed-forward pathway. *Genes Dev*., **24**, 2754-9.

Koturbash, I. *et al*. (2010) Small molecules with big effects: The role of the microRNAome in cancer and carcinogenesis. *Mutation Research*, doi:10.1016/j.mrgentox.2010.05.006.

Elia, L. *et al*. (2009) The knockout of miR-143 and -145 alters smooth muscle cell maintenance and vascular homeostasis in mice: correlates with human disease. *Cell Death Differ*., **16**, 1590-8.

Xin, M. *et al*. (2009) MicroRNAs miR-143 and miR-145 modulate cytoskeletal dynamics and responsiveness of smooth muscle cells to injury. *Genes Dev*., **23**, 2166-78.

Yin, Y. *et al*. (2010) [Expressions of 6 microRNAs in prostate cancer]. *Zhonghua Nan Ke Xue*, **16**, 599-605.

Myatt, S.S. *et al*. (2010) Definition of microRNAs that repress expression of the tumor suppressor gene FOXO1 in endometrial cancer. *Cancer Res*., **70**, 367-77.

Sarver, A.L. *et al*. (2009) Human colon cancer profiles show differential microRNA expression depending on mismatch repair status and are characteristic of undifferentiated proliferative states. *BMC Cancer*, **9**, 401.

Schaefer, A. *et al*. (2010) Diagnostic and prognostic implications of microRNA profiling in prostate carcinoma. *Int J Cancer*, **126**, 1166-76.

Cho, W.C. *et al*. (2009) Restoration of tumour suppressor hsa-miR-145 inhibits cancer cell growth in lung adenocarcinoma patients with epidermal growth factor receptor mutation. *Eur J Cancer*., **45**, 2197-206.

Sacheli, R. *et al*. (2009) Expression patterns of miR-96, miR-182 and miR-183 in the development inner ear. *Gene Expr Patterns*, **9**, 364-70.

Zhang, X. *et al*. (2010) Synergistic effects of the GATA-4-mediated miR-144/451 cluster in protection against simulated ischemia/reperfusion-induced cardiomyocyte death. *J Mol Cell Cardiol*., **49**, 841-50.

Rasmussen, K.D. *et al*. (2010) The miR-144/451 locus is required for erythroid homeostasis. *J Exp Med*., **207**, 1351-8.

Lu, Y. (2009) Amplification and overexpression of Hsa-miR-30b, Hsa-miR-30d and KHDRBS3 at 8q24.22-q24.23 in medulloblastoma. *PLoS One*, **4**, e6159.

Godwin, J.G. (2010) Identification of a microRNA signature of renal ischemia reperfusion injury. *Proc Natl Acad Sci USA*, **107**, 14339-44.

Santhakumar, D. (2010) Combined agonist-antagonist genome-wide functional screening identifies broadly active antiviral microRNAs. *Proc Natl Acad Sci USA*, **107**, 13830-5.

Yin, G. *et al*. (2010) TWISTing stemness, inflammation and proliferation of epithelial ovarian cancer cells through MIR199A2/214. *Oncogene*, **29**, 3545-53.

Magrelli, A. *et al*. (2009) Altered microRNA Expression Patterns in Hepatoblastoma Patients. *Transl Oncol*., **2**, 157-63.

Yang, H. *et al*. (2008) MicroRNA expression profiling in human ovarian cancer: miR-214 induces cell survival and cisplatin resistance by targeting PTEN. *Cancer Res*., **68**, 425-33.

Table S1. Summary of collected function roles of the enriched overlapping miRNAs based on literature search.

No	Function description according to literature abstract	Reference
10	Tumor suppressor function through regulating Rb/E2F1 activity (miR-449a/449b)	Yang *et al*. (2009)
	Targets of p53 and control of cell proliferation and adhesion-independent growth (mir-34b/34c)	Corney *et al*. (2007)
14	Repression of the (miR-143/145 cluster) by oncogenic Ras initiates a tumor-promoting feed-forward pathway	Kent *et al*. (2010)
	Smooth muscle cell (SMC) differentiation and vascular pathogenesis (miR-143/145 cluster)	Elia *et al*. (2009)
	(miR-143/145) modulate cytoskeletal dynamics and responsiveness of smooth muscle cells to injury.	Xin *et al*. (2009)
16	Might be important biomarkers for the early detection and prognostic assessment of prostate cancer	Yin *et al*. (2010)
	Repress FOXO1 expression, affect cell cycle control and apoptotic responses in endometrial cancer	Myatt *et al*. (2010)
	Expression depending on mismatch repair status and characteristic of undifferentiated proliferative states	Sarver *et al*. (2009)
	Upregulated in prostate cancer and useful diagnostic and prognostic indicators	Schaefer *et al*. (2010)
	Differential expressed, related with peculiar tumourigenetic pathways and be potential biomarkers	Cho *et al*. (2009)
	The development of the cochlea (from the patterning to the differentiation of the cochlear structures)	Sacheli *et al*. (2009)
17	Both partners of the (miR-144/451 cluster) confer protection against simulated I/R-induced cardiomyocyte death via targeting CUGBP2-COX-2 pathway	Zhang *et al*. (2010)
	(miR-144/451 cluster) tunes gene expression to impart a robustness to erythropoiesis	Rasmussen *et al*. (2010)
19	Amplification and overexpression of (miR-30b, miR-30d and KHDRBS3) at 8q24.22-q24.23 in medulloblastoma	Lu *et al*. (2009)
20	See 16	See 16
42	Deffiential expressed signature associated with Renal ischemia reperfusion injury (IRI)	Godwin *et al*. (2010)
	miR-199a/miR-214 cluster is down-regulated in both murine and human cytomegalovirus infection and Manifests similar antiviral properties in mouse and human cells	Santhakumar *et al*. (2010)
	Through mir-199a/214, TWISTing stemness, inflammation and proliferation of epithelial ovarian cancer cells	Yin *et al*. (2010)
	Altered microRNA Expression Patterns in Hepatoblastoma Patients	Magrelli *et al*. (2009)
	Deregulation of miRNAs is a recurrent event in human ovarian cancer and that miR-214 induces cell survival and cisplatin resistance primarily through targeting the PTEN/Akt pathway	Yang *et al*. (2008)
46	See 17	See 17

Table S2. Summary of gene modules that are enriched with ovarian cancer genes based on the IPA system. *q*-value, the B-H multiple test corrected *p*-value.

No.	Ovarian cancer genes	genes	*q*-value
2	FN1, INHBA, MMP3, MMP1, POSTN, PTGS2, SERPINE1, VCAN	8	2.87e-02
4	C11ORF9, EFNB2, FGF18, KLK6, KLK8, KLK10, KLK11, SCGB2A1	8	6.06E-02
6	DACH1, EEF1A2, MMP3, S100P, SLIT2, WT1	6	5.73E-02
14	ABCA8, DIRAS3, GSTM5, HSD11B1, ITLN1, MUM1L1	6	4.89E-03
22	DACH1, FAM54A, KPNA2, RRM2, S100P, TOP2A, TYMS	7	5.75E-03
23	CALB2, CFH, CXCL14, FABP4, FGF1, INHBA, PDGFRB, PEG3, POSTN, SLIT2, TIMP3, VCAM1, VCAN	13	1.62E-03
28	DUSP4, EYA2, IFI27, IGFBP1, KLK5, KLK7, KLK8, MMP3, MMP7, PRKCB, S100P, SCGB2A1, VTCN1, WFDC2, WT1	15	4.49E-07
34	CCL4, CSF1R, GPR65, IGFBP1, KLK7, LCN2, MMP7, SCGB2A1	8	2.29E-02
39	FOLR1, HMGA2, HOXB6, KLK11, PROM1, S100A2, TACSTD2, VAV3	8	5.66E-02
40	FAM54A, HIST2H2AA3, KRT23, PAEP, SLPI, TIMP1, TOP2A, VTCN1	8	4.88E-02
42	FLRT2, HOXA4, IGFBP4, KIT, PDGFRA, PEG3, SEMA3C, SERPINA5, TUBB2A	9	3.32E-02
48	CXCL14, FLT1, IL6, INHBA, PLAU, POSTN, TIMP3, VCAN	8	2.20E-03
49	CEACAM6, GPX3, LCN2, PEG3, S100A2, VAV3	6	4.34E-02